Supercond. Sci. Technol. **20** (2007) S128–S135 doi:10.1088/0953-2048/20/9/S03

Pinning size effects in critical currents of superconducting films

A Gurevich

Applied Superconductivity Center, National High Magnetic Field Laboratory, Florida State University, 1800 E Paul Dirac Drive, Tallahassee, FL 32310, USA

Received 1 March 2007, in final form 9 May 2007
Published 23 August 2007
Online at stacks.iop.org/SUST/20/S128

Abstract

The thickness dependence of the critical current density $J_c(d)$ in films due to the two-dimensional–three-dimensional (2D–3D) pinning crossover at low magnetic fields is addressed, taking into account the spatial correlation of pinning centres, the combined effect of bulk and surface pinning, and the effect of thermal fluctuations. The whole $J_c(d)$ curve for both the 3D and 2D pinning regimes, and the crossover thickness d_c are calculated using a dynamic approach for a random pinning potential characterized by the Gaussian correlation functions. It is shown that the spatial correlation of pinning centres can significantly increase d_c as compared to uncorrelated point pins, and the competition between pinning and thermal fluctuations gives rise to a nonmonotonic dependence of $J_c(d)$. The account of multiscale spatial correlations in a uniform pinning nanostructure can result in behaviour of $J_c(d)$ similar to that observed on $YBa_2Cu_3O_{7-\delta}$. The ultimate limit of J_c is discussed.

1. Introduction

Critical current densities J_c of superconducting films are typically much greater than those of bulk superconductors [1–7]. This difference is usually due to denser and stronger pinning defects [8, 9] or artificially introduced nanoprecipitate structures, and the weaker effect of current-blocking obstacles such as grain boundaries, microcracks, etc [10]. It has often (although not always) been observed that $J_c(d)$ first increases as the film thickness d decreases, followed by a decrease of J_c for smaller d. Understanding the mechanisms behind the size dependence of J_c is particularly important for high-T_c multifilamentary conductors and $YBa_2Cu_3O_7$ (YBCO)-coated conductors in which a significant increase of $J_c(d)$ as d decreases has been observed [11–16]. This behaviour of $J_c(d)$ has been attributed to microstructural changes induced by the sample geometry, in particular, 'dead' layers with reduced T_c and J_c or additional pinning due to mismatch dislocations near the buffer layer [2, 11, 12], thickness-dependent grain size structure or porosity [7]. J_c values in films often reach 10–20% of the depairing current density $J_d = c\phi_0/12\sqrt{3}\pi^2\lambda^2\xi$ if d is smaller than the London penetration depth λ, as was observed on NbN multilayers [1], NbTi films [17], or YBCO multilayers [18]. Here ξ is the coherence length, ϕ_0 is the flux quantum, and c is the speed of light.

Besides the thickness-dependent nanostructure, the $J_c(d)$ dependence can also be due to the fact that the pinning of vortices perpendicular to the film surface depends on the vortex length d if it gets smaller than the bulk pinning correlation length L_c along the field direction **H**. Here L_c is determined by the balance of random pinning forces and elastic stresses in the vortex structure [19]. For $d < 2L_c$, a transition from the 3D thickness-independent pinning to the 2D pinning for which $J_c(d)$ increases as d decreases occurs [20–23]. This transition was observed on NbN multilayers [1], Nb_3Ge, Mo_3Si [20, 21] and Mo_xGe_{1-x} [23] films. The 2D pinning may account for the thickness dependence of J_c even for a uniform pinning nanostructure.

The question to what extent the pinning size effects control the behaviour of $J_c(d)$ observed in YBCO films still remains open. For uncorrelated point defects (like oxygen vacancies), the single-vortex collective pinning theory [19] gives $L_c \sim \xi_c\sqrt{J_d/J_c}$ at low fields. Therefore, the 2D pinning occurs for $d < d_c = 2L_c$, where [21]

$$d_c \simeq 2\xi_c\sqrt{J_d/J_c}. \tag{1}$$

Taking the c-axis coherence length, $\xi_c \approx 1$ nm, $J_c \sim 1$ MA cm^{-2} and $J_d \simeq 40$ MA cm^{-2} for a 1 μm YBCO film at 77 K, we get $d_c \approx 10$ nm, much smaller than $d \sim 1$ μm below which YBCO films exhibit a significant increase in $J_c(d)$. Yet,

the result of the collective pinning theory [21], $J_c \propto d^{-1/2}$, actually describes the observed behaviour of $J_c(d)$ in many YBCO films well [11–14]. This inconsistency may indicate that either the pinning size effects are irrelevant or the theory of the 2D–3D pinning should be generalized to take into account multiscale pinning nanostructures of YBCO films. Indeed, the collective pinning theory was originally formulated for the simplest case of point uncorrelated pins. As shown below, d_c can increase to submicron values if the positions of pinning centres are correlated within a domain of size $\sim r_\perp$ much greater than the vortex core radius [24]. In this paper we consider the thickness dependence of $J_c(d)$ in films at low fields for which J_c is determined by single-vortex pinning.

2. 2D–3D pinning crossover

2.1. Surface pinning

The thickness dependence of $J_c(d)$ is often attributed to strong pinning by surface defects [25, 26]. For example, variation of the film thickness $d(x, y)$ causes variation of the vortex self-energy $\varepsilon d(x, y)$, resulting in $J_c = c\varepsilon|\nabla d|/\phi_0 d$ for a straight vortex trapped in a minimum of $d(x, y)$, where ε is the vortex line tension. These models imply that the vortex remains straight as current exerts the Lorentz force to the entire vortex length. However, in this case a vortex pinned at the ends forms an arc with a local curvature radius R determined by the force balance, $\varepsilon/R = J\phi_0/c$. For extremely strong surface pinning, the vortex ends are fixed, and J_c is determined by the condition that the end segments of the vortex line are parallel to the film surface. In this case the vortex gets depinned by reconnecting with its surface image, and [22]

$$J_c = \frac{c\phi_0}{8\pi^2\Gamma\lambda^2 d}\ln\frac{d}{\xi_c}. \tag{2}$$

For a YBCO film with $d = 1$ μm at $T = 77$ K, ($\lambda = 0.3$ μm, the anisotropy parameter $\Gamma = \lambda_c/\lambda = 7$, $\xi_c = 1$ nm), equation (2) gives $J_c \simeq 0.3$ MA cm^{-2}, much smaller than typical values 1–3 MA cm^{-2}. The anisotropy of λ reduces J_c, so the models of straight vortices significantly overestimate J_c. Thus, the observed high values of J_c in YBCO films cannot be explained by only surface pinning without taking into account strong bulk pinning.

2.2. Bulk pinning in films

The pinning size effects in film are particularly transparent at low fields for which displacements of neighbouring vortices are uncorrelated, and $J_c(d)$ can be evaluated using the collective pinning approach [19, 20]. The 2D pinning only causes overall displacements of vortices which remain nearly straight and perpendicular to the film surface. If the film thickness is much greater than the mean pin spacing l_i, the vortex interacts with $N = r_p^2 d/l_i^3 \gg 1$ pins, adjusting its position so that the net pinning force vanishes. Current displaces the vortex from a local potential well, so the balance of the total pinning force $f_p\sqrt{N}$ from uncorrelated pins in the volume $r_p^2 d$ and the Lorentz force $\phi_0 d J/c$ yields $\phi_0 J_c d/c = f_p\sqrt{N}$, whence

$$J_c = \frac{c}{\phi_0}\sqrt{\frac{\gamma}{d}}. \tag{3}$$

Here $\gamma(T, B) = u_p^2 n_i$, $n_i = l^{-1/3}$ is the volume pin density, F_p is an elementary pinning force, r_p is the pin interaction radius and $u_p = f_p r_p$ is the elementary pinning energy. Notice that the $1/\sqrt{d}$ dependence of $J_c(d)$ at low fields turns into the $1/d$ dependence at higher fields [21, 22].

The crossover between the 2D pinning of a rigid vortex to the 3D pinning of a deformable vortex can be evaluated using the collective pinning theory [19]:

$$J_c \sim \frac{c}{\phi_0}\sqrt{\frac{\gamma}{L_c}}, \qquad \epsilon(L_c)\left(\frac{u}{L_c}\right)^2 \sim \frac{\phi_0}{c}uJ_c. \tag{4}$$

The first relation is similar to equation (3) for a vortex segment of length L_c, and the second one reflects the balance of the pinning energy and a bending elastic energy of the vortex segment displaced by u from its equilibrium position. Here the dispersive line tension $\varepsilon(q)$ for the wavevector $q \simeq \pi/L_c$ along the vortex is given by [19]

$$\varepsilon(q) = \frac{\varepsilon_0}{2\Gamma^2}\ln\frac{\lambda_c^2}{\xi^2(1+q^2\lambda^2)} + \frac{\varepsilon_0}{2\lambda^2 q^2}\ln(1+q^2\lambda^2), \tag{5}$$

where $\Gamma = \lambda_c/\lambda = \xi/\xi_c$ is the anisotropy parameter, and $\varepsilon_0 = (\phi_0/4\pi\lambda)^2$ is the scale of the vortex line energy. The strong decrease of $\varepsilon(q)$ from $\sim \varepsilon_0/2$ for $q\lambda \ll 1$ to $\sim \varepsilon_0/\Gamma^2$ for $q\lambda \gg \Gamma$ reflects the essential elastic nonlocality of the vortex line in anisotropic superconductors.

Using the second equation (4) and equation (5), we arrive at the following relation between L_c and J_{c0}:

$$\left(\frac{\pi\lambda}{\Gamma L_c}\right)^2 \ln\frac{\lambda_c^2}{\xi^2[1+(\pi\lambda/L_c)^2]} + \ln\left[1+\left(\frac{\pi\lambda}{L_c}\right)^2\right] = C\frac{\lambda^2}{\xi u}\frac{J_{c0}}{J_d}, \tag{6}$$

where $J_d = 4c\varepsilon_0/3\sqrt{3}\phi_0\xi$ is the Ginzburg–Landau depairing current density in the ab plane. The numerical coefficient $C \sim 1$ cannot be obtained from the qualitative estimate (4), but will be evaluated below from the dynamic theory.

For high J_c caused by uncorrelated point pins ($r_p \sim \xi$, $u \sim \xi$), the right-hand side of equation (6) is much greater than 1 (for instance, $J_c\kappa^2/J_d \sim 10^2$ if $\kappa \simeq 10^2$ and $J_c/J_d \sim 10^{-2}$). Then the first term in the left-hand side dominates, and d_c is given by equation (1). However, for strong pinning centres, the vortex displacements u can be much greater than ξ [28–30], so the term $J_c\kappa\lambda/uJ_d$ in equation (6) can become of the order of unity. In this case L_c may be comparable to λ. This conclusion is illustrated by figure 1 which shows L_c as a function of J_c defined by equation (6) for $\Gamma = 5$ and $\kappa = 100$. Taking, for example, $J_c = 1$ MA cm^{-2}, $J_d = 36$ MA cm^{-2}, $\kappa = 10^2$, $\lambda = 0.3$ μm at 77 K, we obtain that $d_c = 2L_c \simeq 1$ μm corresponds to $L_c/\pi\lambda \simeq 0.5$, which, in turn, requires $J_c\kappa\lambda/uJ_d \simeq 3$, that is, $u \simeq \lambda$. For $L_c > \lambda$ and $\Gamma \gg 1$, the first term in the left-hand side of equation (6) is negligible, so the anisotropy becomes unimportant. Therefore, $d_c = 2L_c$ can significantly exceed the estimate (1) because (1) strong and/or correlated pinning defects cause large vortex displacements $u \gg \xi$, and (2) elastic nonlocality of the vortex line compensates the reduction of d_c due to strong anisotropy for $\Gamma \gg 1$.

The above consideration corresponds to a strong single vortex pinning, for which pinning forces prevail over inter-vortex interactions. This condition can be written in the form

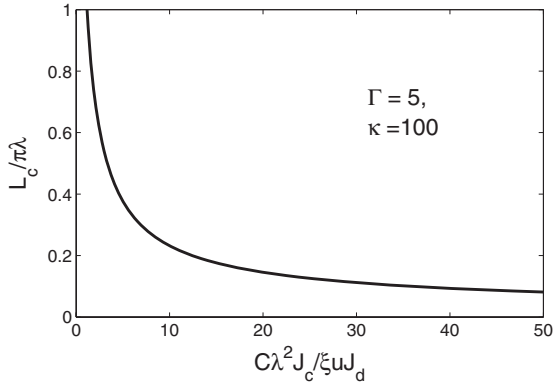

Figure 1. Pinning correlation length L_c defined by equation (6).

$J_c\phi_0/c > Kr_p$, where the spring constant $K = \phi_0 H/8\pi\lambda^2$ results from the magnetic cage potential acting on a vortex from the surrounding amorphous vortex structure. Hence, the single vortex pinning occurs at low fields $H < H_s$, where

$$H_s \simeq 8\pi\lambda^2 J_c/cr_p. \tag{7}$$

It is also assumed that H exceeds the field of full flux penetration $H_p = 4dJ_c/c$, so transport current flow is uniform, vortices are aligned with the applied field perpendicular to the film surface, and the influence of self-field effects and the geometrical barrier [31–33] is negligible. Taking $\lambda(77\ \mathrm{K}) = 0.4\ \mu\mathrm{m}$, $J_c = 4\ \mathrm{MA\,cm^{-2}}$, we obtain $H_p = 64$ Oe and $H_s = 3.2$ T for pins with the interaction radius $r_p = 5$ nm. In the following we consider how spatial correlation of pinning centres affects the thickness dependence of $J_c(d)$ in films for $H_p < H < H_s$.

3. Dynamic J_c in a film

The collective pinning theory was generalized by Kes and Tsui [20] to calculate J_c in films. In this approach strains in the pinned vortex lattice are inhomogeneous over the film thickness, so only asymptotic behaviours of $J_c(d)$ in the 2D ($d \ll d_c$) and 3D ($d \gg d_c$) limits have been obtained [21, 22]. In this work we use the dynamic approach [34] which has been widely applied for the analysis of vortex dynamics and pinning in high-T_c superconductors (HTSs) [19]. Namely, we consider a current-driven vortex and then calculate a dynamic J_c at which the pinning correction $\delta v(J)$ to the vortex velocity becomes comparable to flux flow velocity $v_F = J\phi_0/\eta c$, where η is the vortex viscosity. The dynamic J_c defined by the condition $\delta v(J_c) \simeq v_F(J_c)$ has the same dependence on parameters as the static J_c obtained from the collective pinning force balance [19]. However, in the dynamic approach a closed form equation for $J_c(d)$ can be obtained, which comprises both the 2D and 3D pinning limits, including the crossover region $d \sim d_c$. Another advantage of the dynamic approach is that it can incorporate any form of the correlation function of the pinning potential $F(\mathbf{r}_1, \mathbf{r}_2) = \langle U(\mathbf{r}_1)U(\mathbf{r}_2)\rangle$ to address the effect of the finite correlation lengths and surface pinning.

3.1. Pinning correlation functions

The dynamic J_c can be calculated from the following equation of motion for a single vortex in a random pinning potential $U(\boldsymbol{\rho}, z)$:

$$\eta\dot{\boldsymbol{\rho}} = \int_{-\infty}^{\infty} G(z - z')\boldsymbol{\rho}(z')\mathrm{d}z' - \nabla U(\boldsymbol{\rho}, z) + [\mathbf{J} \times \hat{\mathbf{z}}]\frac{\phi_0}{c} \tag{8}$$

where $\boldsymbol{\rho}(z, t) = (x, y)$ is a local coordinate of the vortex line, the dot denotes the time derivative, and the Fourier transform of the kernel $G(z - z')$, which describes the nonlocal bending rigidity of a vortex, is given by [19]

$$G(q) = \frac{q^2\epsilon_0}{2\Gamma^2}\ln\frac{\lambda^2}{\xi_c^2(1 + q^2\lambda^2)} + \frac{\epsilon_0}{2\lambda^2}\ln(1 + q^2\lambda^2). \tag{9}$$

The statistical properties of $U(\mathbf{r}, z)$ are defined by the averages $\langle U\rangle = 0$, and by the correlation functions

$$\langle U(\mathbf{r}_1)U(\mathbf{r}_2)\rangle = F_b(|\boldsymbol{\rho}_1 - \boldsymbol{\rho}_2|, z_1 - z_2) + F_s(|\boldsymbol{\rho}_1 - \boldsymbol{\rho}_2|)p(z_1)p(z_2). \tag{10}$$

Here $\langle U(\mathbf{r}_1)U(\mathbf{r}_2)\rangle$ contains the bulk part F_b and the part F_s localized near the surfaces, where $\mathbf{r} = (\boldsymbol{\rho}, z)$, the coordinate $\boldsymbol{\rho}$ lies in the film plane, and the z-axis is perpendicular to the film surface. Equation (10) describes the situation in which the surface pinning is different from the bulk one. The pinning potential in the xy plane is assumed statistically uniform and isotropic, and $p(z)$ describes the decay of the surface component on the length $\sim l$. In this work the Gaussian correlators are used:

$$F_b(\rho, z) = F_{b0}\exp\left(-\frac{\rho^2}{r_\perp^2} - \frac{z^2}{r_\parallel^2}\right), \tag{11}$$

$$F_s(\rho) = F_{s0}\exp(-\rho^2/r_s^2), \qquad p(z) = \mathrm{e}^{-z/l}, \tag{12}$$

where F_{b0} and F_{s0} quantify the strength of bulk and surface pinning, respectively, $r_\perp$ and $r_\parallel$ are bulk correlation radii of the pinning potential in the xy plane and along the z-axis, and r_s is the correlation radius of the surface pinning potential localized in the layer of thickness l at the film surface. Here $r_\perp$, $r_\parallel$, r_s and l are generally controlled by different mechanisms. For example, in HTSs the difference in $r_\parallel$ and $r_\perp$ reflects the crystal anisotropy, while r_s may quantify the scale of the surface roughness. The separation of $\langle U(\mathbf{r}_1)U(\mathbf{r}_2)\rangle$ into the bulk and surface components is justified if $r_\parallel$ and $r_\perp$ are much smaller than the film thickness. The case $l \ll d$ describes pinning defects localized at the surface (for example, interface dislocations [11, 12]), while the case $l > d$ corresponds to correlated defects, such as threading dislocations [35] or radiation columnar defects [36] or linear artificial pinning centres (nanorods) [37, 38] perpendicular to the film surface, but randomly distributed in the film plane.

To illustrate the length scales of the pinning correlation functions, we consider an array of identical pins, each interacting with a vortex via the potential $u(\mathbf{r})$. Then the global pinning potential is

$$U(\mathbf{r}) = \int u(\mathbf{r} - \mathbf{R})[n(\mathbf{R}) - n_i]\,\mathrm{d}^3\mathbf{R}, \tag{13}$$

where $n(\mathbf{R}) = \sum_n \delta(\mathbf{R} - \mathbf{R}_n)$ is a local density of pins, $n_i = \langle n\rangle$, and $\delta n(\mathbf{r}) = n(\mathbf{r}) - n_i$ is the density fluctuation.

Using equation (13), the correlation function $F(\mathbf{r}-\mathbf{r}') = \langle U(\mathbf{r})U(\mathbf{r}')\rangle$ for a macroscopically uniform distribution of pinning centres can be written in the form

$$F(\mathbf{r}-\mathbf{r}') = \int \frac{\mathrm{d}^3\mathbf{k}}{(2\pi)^3}|u(\mathbf{k})|^2 S(\mathbf{k})\mathrm{e}^{\mathrm{i}\mathbf{k}(\mathbf{r}-\mathbf{r}')}, \qquad (14)$$

where $u(\mathbf{k})$ is the Fourier transform of $u(\mathbf{r})$, and $S(\mathbf{k})$ is the Fourier transform of the pin density correlation function

$$S(\mathbf{k}) = \int \mathrm{d}^3\mathbf{r}\,\mathrm{e}^{-\mathrm{i}\mathbf{k}\mathbf{r}}\langle\delta n(\mathbf{r})\delta n(0)\rangle, \qquad (15)$$

normalized by the condition $\int S(\mathbf{r})\mathrm{d}^3\mathbf{r} = n_i$. Here we take the Gaussian structural factor,

$$S(\mathbf{r}) = \frac{n_i}{\pi^{3/2}l_\perp^2 l_\parallel}\exp\left(-\frac{\rho^2}{l_\perp^2}-\frac{z^2}{l_\parallel^2}\right), \qquad (16)$$

where $\rho^2 = x^2+y^2$, and $l_\perp$ and $l_\parallel$ define the spatial extent over which positions of pinning centres are statistically correlated (for example due to elastic interaction of precipitates). Because of the HTS anisotropy, $l_\perp$ in the ab plane may differ from $l_\parallel$ along the c-axis.

Now we consider different forms of the elementary pinning potential $u(r)$, starting from a short-range core interaction approximated by [19]

$$u(\rho,z) = \frac{u_\mathrm{p}}{r_0\sqrt{\pi}}\exp\left(-\frac{\rho^2+z^2}{r_0^2}\right), \qquad (17)$$

where r_0 is the size of a precipitate or a region of reduced T_c, and $u_\mathrm{p} = \int_{-\infty}^{\infty}u(0,z)\mathrm{d}z$ is the total pinning energy. Substituting equations (16) and (17) into (14) yields (11), in which $F_{\mathrm{b}0} = n_i u_\mathrm{p}^2\sqrt{\pi}r_0^4/r_\perp^2 r_\parallel$, and

$$r_\perp = (2r_0^2+l_\perp^2)^{1/2}, \qquad r_\parallel = (l_\parallel^2+2r_0^2)^{1/2}. \qquad (18)$$

Another example is the attraction force density $f(\rho,z)$ per unit vortex length produced by a small insulating precipitate or by a pore of radius $r_0 \ll \lambda$ spaced by $\rho < \lambda$ from the vortex. Pinning by nanopores in YBCO films has been recently discussed by several groups [7, 39]. The force $f(\rho,z)$ calculated in appendix A has the form

$$f(\rho,z) \simeq \frac{\epsilon_0 r_0^3}{(\rho^2+r_0^2)^{1/2}(\rho^2+z^2+r_0^2)^{3/2}}. \qquad (19)$$

Equation (19) gives the total pinning force, $f_\mathrm{p}(\rho) = \int_{-\infty}^{\infty}f(\rho,z)\mathrm{d}z = 2\epsilon_0 r_0^3/(\rho^2+r_0^2)^{3/2}$, and the pinning energy, $u_\mathrm{p} = \int_0^\infty f_\mathrm{p}(\rho)\mathrm{d}\rho = 2\epsilon_0 r_0$. Here r_0 in the denominator qualitatively provides a smooth transition to the vortex–pore interaction at short distances [40]. Thus, both the long-range magnetic pinning interaction described by equation (19) and the short-range core pinning modelled by equation (17) can produce very high pinning energies $u_\mathrm{p} \simeq 2r_0\epsilon_0$ equal to the gain in the condensation core energy of a vortex segment in the pore.

If the pin interaction radius is comparable to the radius $l_\perp$ of the domain where the positions of pins are correlated, $F(\mathbf{r}-\mathbf{r}')$ depends on the particular forms of both $u(r)$ and $S(r)$. For the magnetic force (19), as well as long-range interactions between vortices and grain boundaries [41] or columnar defects [42], the pinning correlation function $F(\mathbf{r}-\mathbf{r}')$ is far from being Gaussian even for the Gaussian structural factor $S(r)$. However, for $l_\perp \gg r_0$, the behaviour of $F(\mathbf{r}-\mathbf{r}')$ is mostly determined by $S(r)$, while the shape of $u(r)$ only affects the amplitude $F_{\mathrm{b}0}$. So the convenient Gaussian approximations (11) and (12) are used here for the calculation of $J_\mathrm{c}(d)$, although, unlike short-range pins, the amplitudes $F_{\mathrm{c}0}$ and $F_{\mathrm{s}0}$ for the long-range pinning interaction cannot be readily expressed in terms of the pinning energies u_p.

3.2. *Thickness dependence of J_c*

Calculation of the dynamic J_c for the Gaussian pinning correlation functions (11) and (12) presented in appendix B, results in the following equation for $J_\mathrm{c}(d)$

$$J_\mathrm{c}^2 \simeq \frac{8c^2}{\phi_0^2}\sum_{n=0}^{\infty}\left[\frac{\sqrt{\pi}r_\parallel F_{\mathrm{b}0}}{dr_\perp^2}\mathrm{e}^{-k_n^2 r_\parallel^2/4}Q\left(\frac{cr_\perp G_n}{\phi_0 J_\mathrm{c}}\right)\right.$$
$$\left.+\frac{2l^2F_{\mathrm{s}0}[1-(-1)^n\mathrm{e}^{-d/l}]^2}{(1+\delta_{n0})(1+l^2k_n^2)^2d^2r_\mathrm{s}^2}Q\left(\frac{cr_\mathrm{s}G_n}{\phi_0 J_\mathrm{c}}\right)\right], \qquad (20)$$

where $G(k_n)$ is defined by equation (9), and

$$Q(s) = \int_0^\infty \mathrm{e}^{-t^2-st}(2t-t^3)\,\mathrm{d}t. \qquad (21)$$

Here $Q(s) \approx 2/(4+1.1s+s^2)$ to an accuracy $\simeq$6%. The two terms in the brackets in equation (20) represent contributions from bulk and surface pinning, respectively. The case $l \ll d$ corresponds to the localized surface pinning, and the case $l \gg d$ models pining by linear defects.

For small d, the vortex bending modes with $n \neq 0$ can be neglected, and the sum in equation (20) is dominated by the term with $n = 0$. This case corresponds to the 2D pinning for which equation (20) yields for $l \ll d$

$$J_\mathrm{c} = \frac{c}{\phi_0}\left(\frac{\gamma_\mathrm{b}}{d}+\frac{\gamma_\mathrm{s}l}{d^2}\right)^{1/2} \qquad (22)$$

where $\gamma_\mathrm{b} = 4\sqrt{\pi}r_\parallel F_{\mathrm{b}0}/r_\perp^2$, and $\gamma_\mathrm{s} = 4F_{\mathrm{s}0}l/r_\mathrm{s}^2$. If surface pinning is negligible, equation (22) reduces to the collective pinning estimate (3) with $\gamma_\mathrm{b} = 4\pi u_\mathrm{p}^2 n_i (r_0/r_\perp)^4$ for the short-range pins described by equation (17). As follows from equation (22), the squared critical current $I_\mathrm{c} = J_\mathrm{c}dw$ is a linear function of the film thickness:

$$I_\mathrm{c}^2 = (\gamma_\mathrm{b}d+\gamma_\mathrm{s}l)\,(cw/\phi_0)^2. \qquad (23)$$

This form is convenient for separating bulk and surface pinning contributions from the observed $I_\mathrm{c}(d)$, and to reveal the effect of a 'dead layer' for which $\gamma_\mathrm{s} < 0$. Equation (23) is also useful for distinguishing the 2D collective pinning from the 3D pinning in a film with an extra surface pinning. In the latter case, $J_\mathrm{c}(d) = J_{\mathrm{c}0}(1+d_\mathrm{s}/d)$, so $I_\mathrm{c}(d)$ is a linear function of d, where w is the film width and $J_{\mathrm{c}0}$ is the bulk critical current density.

Equation (20) describes the dimensional crossover from the 2D to 3D pinning produced by the vortex bending modes with $n > 0$. We consider this transition in more detail, neglecting surface pinning ($\gamma_\mathrm{s} = 0$). The 2D mode with $n = 0$ dominates if the functions $Q(cr_\perp G_n/\phi_0 J_\mathrm{c})$ in

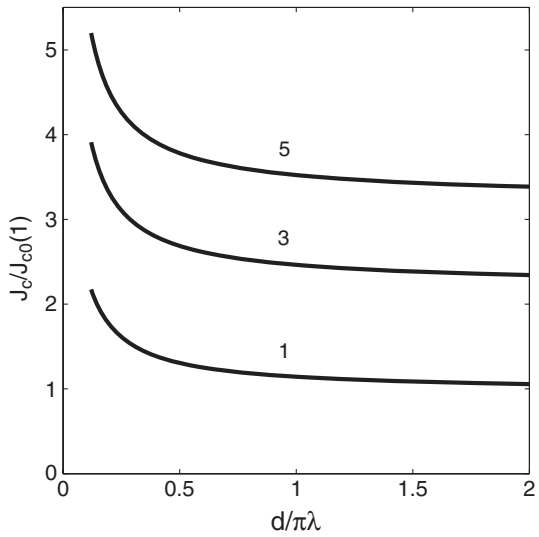

Figure 2. $J_c(d)$ calculated from equation (20) with no surface pinning for different values of the dimensionless pinning parameter $g = 32r_\parallel\lambda^3 F_{b0}/\sqrt{\pi}r_\perp^4\varepsilon_0^2 = 1$, 3 and 5, and $r_\parallel = 0.1\lambda$. All J_c values are normalized to J_{c0} for the 3D pinning at $g = 1$.

equation (22) rapidly decrease with n, so the critical thickness d_c is determined by the condition $cr_\perp G_1/\phi_0 J_c \simeq 1$. This condition does reduce to equation (6) with $u = r_\perp$ and $C = 8/3\sqrt{3}$. Therefore, the dynamic approach not only reproduces the results of collective pinning analysis, but also shows that the relevant vortex displacement u in equation (6) equals the correlation radius $r_\perp$, which can be much greater than ξ. Thus, d_c can be much greater than the estimate (1) for uncorrelated point pins, as discussed above. In the 3D regime, $d \gg d_c$, the summation of the slowly varying Q functions in equation (3) can be replaced by integration, which reproduces the well-known results of the collective pinning theory for J_c in the limit of uncorrelated pins, $F(\mathbf{r} - \mathbf{r_1}) \to \gamma\delta(\mathbf{r} - \mathbf{r}_1)$ [19].

Shown in figure 2 is the full dependence of $J_c(d)$ calculated from equation (20). A convenient interpolation of $J_c(d)$ without surface pinning is given by

$$J_c(d) = J_{c0}\sqrt{1 + \frac{d_c}{d}} \tag{24}$$

where the 3D pinning J_{c0} corresponds to $d \gg d_c$. Equation (24) approximates the $J_c(d)$ curve in figure 2 to an accuracy $\simeq$3–4%. For the values of the parameters given in the caption of figure 2, the crossover thickness $d_c \simeq 0.5\pi\lambda$ is about 0.6 μm for YBCO at 77 K. Here d_c can be extracted from experimental data by plotting $I_c^2/d \propto d + d_c$. Notice that increasing the pinning strength parameter g defined in the caption of figure 2 mostly increases the magnitude of $J_c(d)$, but has little effect on d_c.

4. Effect of thermal fluctuations

Pinning size effects also affect the thermally activated vortex dynamics, which determines the E–J characteristics and the irreversibility field in HTSs. Thermal fluctuations are most pronounced in thin films for which they can significantly change the thickness dependence of $J_c(d)$ for the 2D collective pinning. We illustrate here the mechanisms by which fluctuations affect $J_c(d)$ in a simple but exactly solvable model. In the flux creep region, $J < J_c$, the small electric field E is mostly determined by rare thermally activated jumps of vortices between pinning wells in the direction of the Lorentz force. Since vortices in thin films basically behave like particles, one can qualitatively consider an effective 1D dynamics of a vortex in a 'washboard' potential

$$d\eta\,\dot{x} = d\phi_0\, J/c - P\sin kx + \zeta. \tag{25}$$

Here $P = dJ_c\phi_0/c$ is the maximum pinning force, $\ell = 2\pi/k$ is a spacing between potential wells, ζ is the white noise thermal force, and the pinning size effects manifest themselves in the dependence of $P(d)$, say $P \propto d(1+d_c/d)^{1/2}$ for the 2D–3D pinning crossover in equation (24) and $P \propto (d + d_s)^{1/2}$ for the 2D pinning, where $d_s = l\gamma_s/\gamma_b$. Equation (25) is analogous to the equation for an overdamped point Josephson junction, for which $E(J)$ can be calculated exactly [43]. Equation (25) has also been used to describe the thermally activated dynamics of vortices [44, 45]. The E–J characteristics in this model has the form

$$\epsilon = \theta(1 - \mathrm{e}^{-\pi\beta t/\theta})/t \int_0^\pi \mathrm{e}^{-\beta t\alpha/\theta} I_0\left[\frac{f(t)\sin\alpha}{\theta}\right] \mathrm{d}\alpha, \tag{26}$$

where $\epsilon = E/\rho_F J_0$, $\beta = J/J_{c0}$, $t = d/d_c$, and $f(t) = P(d)/P(d_c)$ are the dimensionless electric field, current density, film thickness and pinning force, respectively, $\rho_F = \rho_n H/H_{c2}$ is the flux flow resistivity, $I_0(x)$ is a modified Bessel function, and the dimensionless temperature θ quantifies the strength of thermal fluctuations:

$$\theta = \pi k_B cT/J_{c0}\phi_0 d_c \ell. \tag{27}$$

For $J_{c0} = 1$ MA cm^{-2}, $d_c = 0.5$ μm, $\ell = 50$ nm and $T = 77$ K, equation (27) yields $\theta \simeq 6.7 \times 10^{-3}$.

For a given electric field criterion $\epsilon_c = E_c/\rho_F J_{c0}$, the implicit equation (26) determines the thickness dependence of J_c with the account of thermally activated vortex hopping. Shown in figure 3 is the evolution of $J_c(t)$ calculated from the equation $\epsilon_c = \epsilon[J_c(t)]$ for $f(t) = \sqrt{t(1+t)}$ given by equation (24) and $\epsilon_c = 10^{-6}$ for $E_c = 1$ μV cm^{-1}, $B/B_{c2} = 0.01$, and $\rho_n = 0.1$ mΩ cm^{-1}. The $J_c(d)$ curves are plotted for different values of the parameter θ, which increases as either T or B increases, and $J_{c0}(T, B)$ in equation (27) decreases.

As follows from figure 3, the interplay of pinning and thermal fluctuations can produce a maximum in $J_c(t)$, which disappears for larger θ. For small θ, thermal fluctuations do not affect the 2D thickness dependence $J_c \propto d^{-1/2}$, except for very small d. This effect is rather transparent: as the vortex length in thinner films decreases, the 2D pinning becomes stronger, but vortex fluctuations which average out the pinning potential also become stronger, eventually causing the drop of $J_c(d)$. The behaviour of $J_c(d)$ for small d depends on what pinning mechanism dominates. For weak surface pinning, the amplitude of vortex fluctuations $u_\theta = (k_B T/Pk)^{1/2}$ increases as d decreases, so $J_c(d)$ in figure 3 vanishes as $d \to 0$. If, however, surface pinning dominates, both the spring constant Pk and the transport $J_c(d)$ remain finite even for $d \to 0$, and the peak in $J_c(d)$ can disappear.

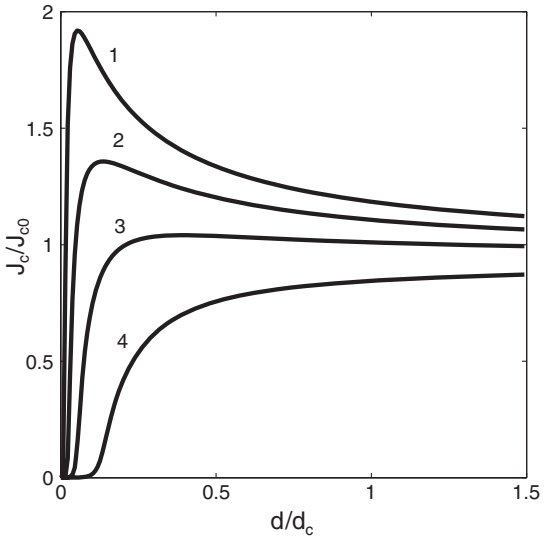

Figure 3. Evolution of the thickness dependence of $J_c(d)$ described by equation (26) for different values of (1) $\theta = 0.0065$, (2) 0.01, (3) 0.015, and (4) 0.025.

5. Discussion

This work shows that a significant thickness dependence of J_c due to the 2D–3D collective pinning crossover can occur below d_c that is much greater than what follows from equation (1) if the positions of the pinning centres are correlated. Such short-range order may, for example, result from elastic interaction of pinning centres during the film growth. In fact, there is no *a priori* reason that pinning centres are completely uncorrelated down to the scale $\sim \xi$, as is usually assumed in the collective pinning theory [19]. However, although the thickness dependence (24) is rather universal and describes the observed dependences of $J_c(d)$ in some YBCO films well [11–14], the particular value of d_c may vary from sample to sample. As follows from figure 2, the higher J_{c0} is, the less pronounced the thickness dependence of J_c is.

Thermal fluctuations can modify the behaviour of $J_c(d)$, as illustrated by figure 3. For small values of the parameter θ (at low H and T), the dependence $J_c(d)$ predicted by the 2D collective pinning model remains practically unchanged except for very small d, where a maximum in $J_c(d)$ develops. As T and/or H increases, the $J_c(d)$ curves flatten out; the maximum in $J_c(d)$ shifts toward larger d, and eventually disappears. A qualitatively similar trend was observed on YBCO films [15] as T was increased from 13 to 65 K. In addition, thermal fluctuations reduce the irreversibility field in thinner films, which is another fingerprint of the 2D collective pinning scenario.

The manifestations of the 2D pinning and thermal fluctuations in $J_c(d)$ may occur only if a vortex line is collectively pinned by many comparatively weak defects to produce high J_c values. Stronger and larger pins like insulating nanoprecipitates which turned out to be very effective in increasing J_c of YBCO films at higher magnetic fields [4, 5] can subdivide a vortex line into weakly coupled segments pinned independently. In this case no strong thickness dependence of $J_c(d)$ is expected because the length of vortex segments is of order of pin separation ($\sim$10–10^2 nm), much smaller than the film thicknesses. Such a situation may occur in YBCO films produced by metal–organic deposition [7]. Yet, the 2D–3D pinning scenario predicts that the behaviour of $J_c(d)$ can be changed by varying T and B. This feature enables one to experimentally distinguish it from the behaviour of $J_c(d)$ controlled by a thickness-dependent microstructure.

Since J_c increases as d decreases, one can pose the question of what maximum J_{cm} can be reached by reducing the pin spacing l_i in the extreme strong pinning limit. For a sparse pinning structure, J_c always increases as the pin density increases; however, as l_i becomes of the order of the core size, insulating pinning nanoprecipitates start blocking the current and $J_c(l_i)$ decreases. As a result, J_c reaches the maximum J_{cm} at the optimum volume fraction of pins x_m determined by the competition between pinning and current-blocking effects. A rough estimate of J_{cm} at low fields can be made by considering pin breaking for a vortex segment between two very strong pins spaced by $L_\perp$ along the c-axis. At $J = J_c$ such a segment forms a critical elliptic loop of width $L_\perp$ along the c-axis and of length $L_\parallel = L_\perp\Gamma$ along the current flowing in the ab plane [27]. The condition that this loop can squeeze between pinning centres, $L_\parallel L_\perp \sim l_i^2$, defines the critical length of vortex segments $L_\perp \sim l_i/\sqrt{\Gamma}$ for randomly distributed pins. Now J_c can be estimated using equation (2) in which d is replaced with the loop width $L_\perp \sim l_i/\sqrt{\Gamma}$:

$$J_c \simeq \frac{c\phi_0 \ln(l_i\sqrt{\Gamma}/\xi)}{8\pi^2\lambda^2 l_i\sqrt{\Gamma}}\left(1 - \frac{4\pi r_0^3}{3l_i^3 x_c}\right). \qquad (28)$$

Here the last factor in the parentheses accounts for the reduction of the current-carrying cross section $A_{eff} = (1 - x/x_c)A$ in the effective medium theory [7], $x = 4\pi r_0^3/3l_i^3$ is the volume fraction of insulating pins of radius r_0, and x_c is the percolation threshold. The function $J_c(x)$ reaches the maximum at $x_m \simeq x_c/4$. If we take the 2D percolation threshold $x_c = 0.5$ for an anisotropic HTS and $\Gamma = 7$, the numerical optimization of equation (28) gives $l_m = 3.75r_0$, $x_m \approx 8\%$, $J_{cm} \approx 0.5J_d$ for $r_0 = \xi$, and $l_m \approx 3.6r_0$, $x_m \approx 9\%$, $J_{cm} \approx 0.33J_d$ for $r_0 = 2\xi$, and $l_m = 3.54r_0$, $x_m \approx 9.5\%$, $J_{cm} \approx 0.25J_d$ for $r_0 = 3\xi$. Notice that r_0 may exceed the geometrical radius of the precipitate if superconductivity at the interface is suppressed by strains, local hole depletion, etc. These estimates show a clear trend for the limit to which J_c can be increased by adding nanoprecipitates, giving the optimum J_{cm} at $\approx$10% volume fraction of pins, consistent with the observations by Haugan *et al* [4] on YBCO films. The fundamental mechanisms, which control the limit of in-field J_c, and the irreversibility field for strong pinning are still poorly understood. However, the observed radical enhancement of in-field J_c by insulating nanoparticles shows a very effective route to this problem.

Acknowledgments

This work was partly supported by AFOSR. The work at NHMFL is supported by NSF Grant DMR-0084173 with support from the state of Florida.

Appendix A. Pinning by a pore

The superfluid velocity distribution $\mathbf{v}(\mathbf{r}) = \mathbf{J}/ne^2$ around a sphere or radius r_0 has the form [46]

$$\mathbf{v} = [3\mathbf{n}(\mathbf{Vn}) - \mathbf{V}]r_0^3/2r^3. \tag{A.1}$$

Here $\mathbf{n} = \mathbf{r}/r$, and $\mathbf{V}$ is the velocity of external uniform flow. We assume that V results from the circulating current density of a vortex line, $J(\rho) = c\phi_0/8\pi^2\lambda^2\rho$ at the distance $\rho < \lambda$ from the pore, where the London screening is ineffective, and $J(r)$ varies weakly over lengths $\sim r_0$. The magnetic interaction force results from the Lorentz force caused by the pore-induced disturbance of the velocity component perpendicular to the vortex line. Since $\mathbf{Vn} = 0$ for any $\mathbf{r}$ connecting the pore and the vortex, the Lorentz force per unit length $\mathbf{f} = [\mathbf{J} \times \mathbf{z}]\phi_0/c$ only comes from the second term in the brackets in equation (A.1), giving $f(\rho, z) = \phi_0^2 r_0^3/16\pi^2\lambda^2\rho(\rho^2 + z^2)^{3/2}$. For smaller distances, $\rho \sim r_0$, the uniform flow approximation fails, but a simple regularization $\rho^2 \to \rho^2 + r_0^2$ provides a qualitative interpolation between the asymptotic equation (19) for $r_0 \ll \rho \ll \lambda$ and the vortex sitting on the pore ($\rho \sim r_0$) for which the pinning energy $u_\mathrm{p} \sim r_0\varepsilon_0$ [40].

Appendix B. Dynamic approach

For a rapidly moving vortex, $\boldsymbol{\rho}(t, z) = \mathbf{v}t + \mathbf{u}(z, t)$, where $\mathbf{v} = [\mathbf{J} \times \mathbf{z}]\phi_0/c\eta$, and $\mathbf{u}(z, t)$ is a vortex distortion,

$$\delta\mathbf{r}(z, t) = \sum_{n=-\infty}^{\infty} \mathbf{A}_n(t) \cos k_n z. \tag{B.1}$$

Here the term with $n = 0$ describes the displacement of the rigid vortex due to pinning, and the terms with $n > 0$ correspond to elastic bending modes with the wavevectors $k_n = \pi n/d$, which ensure that the vortex ends are perpendicular to the film surface. Equation (8) is solved in perturbations in $\delta v/v$:

$$\eta\dot{\mathbf{u}}(z, t) = \int_{-\infty}^{\infty} G(z - z_1)\mathbf{u}(z_1, t)\mathrm{d}z_1 - \nabla U_0(t, z), \tag{B.2}$$

where $U_0(t, z) = U(x_0 - vt, y_0, z)$. From equations (B.1) and (B.2), we obtain

$$\mathbf{u}(z, t) = -\frac{1}{\eta d} \sum_{n=-\infty}^{\infty} \cos k_n z \mathrm{e}^{-\omega_n t} \times \int_{-\infty}^{t} \mathrm{d}t_1 \int_0^d \mathrm{e}^{\omega_n t_1} \cos k_n z_1 \nabla U_0 \mathrm{d}z_1, \tag{B.3}$$

where $\omega_n = G(k_n)/\eta$, and $G(k_n)$ is given by equation (9). Next $\delta\mathbf{v}$ is calculated, expanding U in equation (8) in $\mathbf{u}$, integrating over z and averaging over the pinning disorder:

$$\delta v = \frac{1}{d\eta} \int_0^d [\langle u_x \partial_{xx}^2 U\rangle + \langle u_y \partial_{xy}^2 U\rangle]\mathrm{d}z, \tag{B.4}$$

where $x(t) = x_0 - vt$, and $y = y_0$. Combining equation (B.3) into (B.4) gives

$$\delta v = \frac{1}{d^2\eta^2} \sum_{n=-\infty}^{\infty} \int_{-\infty}^{t} \mathrm{d}t_1 \mathrm{e}^{\omega_n(t_1 - t)} \int_0^d \mathrm{d}z \int_0^d \mathrm{d}z_1 \times \cos k_n z \cos k_n z_1 \left[\partial_{xxx}^3 F + \partial_{xyy}^3 F\right]_{x = v(t_1 - t)}. \tag{B.5}$$

Inserting F defined by equations (10)–(12) with $x - x_1 = v(t - t_1)$ and $y - y_1 \to 0$ into equation (B.5), and integrating over z, z_1 and t_1, yields

$$v = \frac{J\phi_0}{\eta c} - \frac{8c}{\eta\phi_0 J} \sum_{n=0}^{\infty} \left[\frac{\sqrt{\pi} r_\parallel F_{\mathrm{b}0}}{\mathrm{d}r_\perp^2} \mathrm{e}^{-k_n^2 r_\parallel^2/4} Q\left(\frac{cr_\perp G_n}{\phi_0 J}\right) + \frac{2l^2 F_{\mathrm{s}0}[1 - (-1)^n \mathrm{e}^{-d/l}]^2}{d^2 r_\mathrm{s}^2 (1 + \delta_{n0})(1 + l^2 k_n^2)^2} Q\left(\frac{cr_\mathrm{s} G_n}{\phi_0 J}\right)\right], \tag{B.6}$$

where $Q(s)$ is defined by equation (21). The condition $v(J_\mathrm{c}) = 0$ results in equation (20).

References

[1] Gray K E, Kampwirth R T, Murduck J M and Capone D W 1988 *Physica* C **152** 445
[2] MacManus-Driscoll J L *et al* 2004 *Nat. Mater.* **3** 439
[3] MacManus-Driscol J L *et al* 2005 *Appl. Phys. Lett.* **86** 032505
[4] Haugan T J, Barnes P N, Wheeler R, Meisenkothen F and Sumption M D 2004 *Nature* **430** 867
[5] Yoshida Y *et al* 2005 *Japan. J. Appl. Phys.* **44** L546
[6] Obradors X *et al* 2006 *Supercond. Sci. Technol.* **19** S13
[7] Kim S I, Gurevich A, Song X, Li X, Rupich M W, Holesinger T G and Larbalestier D C 2006 *Supercond. Sci. Technol.* **19** 968
[8] Campbell A M and Evetts J E 1972 *Adv. Phys.* **21** 194
[9] Hilton T L and Beasley M R 1990 *Phys. Rev.* B **41** R11669
[10] Larbalestier D C, Gurevich A, Feldmann D M and Polyanskii A 2001 *Nature* **414** 368
[11] Foltyn S R, Jia Q X, Arendt P N, Kinder L, Fan Y and Smith J F 1999 *Appl. Phys. Lett.* **75** 3692
[12] Civale L *et al* 2004 *J. Low Temp. Phys.* **135** 87
[13] Paranthaman M *et al* 2000 *J. Mater. Res.* **15** 2647
[14] Ijaduola A O, Thompson J R, Feenstra R, Christen D K, Gapud A A and Song X 2006 *Phys. Rev.* B **73** 134502
[15] van der Beek C J *et al* 2002 *Phys. Rev.* B **66** 024523
[16] Matsushita T, Kiuchi M, Kimura K, Miyata S, Ibi A, Miroga T, Yamada Y and Shiohara Y 2006 *Supercond. Sci. Technol.* **18** S227
[17] Stejic G, Gurevich A, Kadyrov E, Christen D, Joynt R and Larbalestier D C 1994 *Phys. Rev.* B **49** 1247
[18] Foltyn S R *et al* 2005 *Appl. Phys. Lett.* **87** 162505
[19] Blatter G, Feigelman M V, Geshkenbein V B, Larkin A I and Vinokur V M 1994 *Rev. Mod. Phys.* **66** 1125
[20] Kes P H and Tsuei C C 1983 *Phys. Rev.* B **28** 5126
[21] Kes P H and Wördenweber R 1987 *J. Low Temp. Phys.* **67** 1
[22] Brandt E H 1986 *J. Low Temp. Phys.* **64** 375
[23] Garten F, White W R and Beasley M R 1995 *Phys. Rev.* B **51** 1318
[24] Gurevich A 2004 *Annual DOE Peer Review (Washington DC, July)*
[25] Joss Ch, Forkl A, Warthmann R, Habermeier H-U, Leibold B and Kronmüller H 1996 *Physica* C **266** 235
[26] Kosse A I *et al* 2003 *Pis. Zh. Eksp. Teor. Fiz.* **78** 832
Kosse A I *et al* 2003 *JETP Lett.* **78** 379 (Engl. Transl.)
[27] Brandt E H 1992 *Phys. Rev. Lett.* **69** 1105
[28] Labusch R 1969 *Cryst. Lattice Defects* **1** 1
[29] Ovchinnikov Yu N and Ivlev B I 1991 *Phys. Rev.* B **43** 8024
[30] Blatter G, Geshkenbein V B and Koopmann J A G 2004 *Phys. Rev. Lett.* **92** 067009
[31] Brandt E H and Indenbom M V 1994 *Phys. Rev.* B **48** 12893
[32] Zeldov E, Clem J R, McElfresh M and Darwin M 1994 *Phys. Rev.* B **49** 9802
[33] Zeldov E, Larkin A I, Geshkenbein V B, Konczykowski M, Mayer D, Khaykovich B, Vinokur V M and Shtrikman H 1994 *Phys. Rev. Lett.* **73** 1428
[34] Schmidt A and Hauger W 1973 *J. Low Temp. Phys.* **11** 667
[35] Huijbregtse J M *et al* 2000 *Phys. Rev.* B **62** 1338
[36] Civale L 1977 *Supercond. Sci. Technol.* **10** A11

[37] Matsumoto K, Horide T, Ichinose A, Horrii S, Yoshida Y and Mukaida M 2005 *Japan. J. Appl. Phys.* **44** L246
[38] Goyal A *et al* 2005 *Supercond. Sci. Technol.* **18** 1533
[39] Emergo R L S, Wu J Z, Aytug T and Christen D K 2004 *Appl. Phys. Lett.* **85** 618
[40] Friedel J, de-Gennes P G and Matricon J 1963 *Appl. Phys. Lett.* **2** 199
[41] Gurevich A and Cooley L D 1994 *Phys. Rev.* B **50** 13563
[42] Mkrtchyan G S and Shmidt V V 1971 *Zh. Exp. Teor. Fiz.* **61** 367
Mkrtchyan G S and Shmidt V V 1972 *Sov. Phys.—JETP* **34** 195 (Engl. Transl.)
[43] Ambegaokar V and Halperin B I 1969 *Phys. Rev. Lett.* **22** 1364
[44] Soulen R J *et al* 1994 *Phys. Rev.* B **50** 478
[45] Le Doussal P and Vinokur V M 1995 *Physica* C **254** 63
[46] Lamb H 1945 *Hydrodynamics* (New York: Dover)